Mechanics Modelling of Eccentrically Arranged Concentric Tubes

Z. Mitros[1], M. Khadem[1], C. Seneci[1], L. DaCruz[1,2*], and C. Bergeles [1,2*]

[1] *Wellcome/EPSRC Centre for International and Surgical Sciences, UCL, London*

[2] *UCL Institute of Ophtalmology*

*zisos.mitros.17@ucl.ac.uk , *Equal Senior Authorship*

INTRODUCTION

Continuum robots allow accessing surgical targets deep inside the human body by steering along 3D curves in confined spaces. Further, they provide enhanced dexterity compared to traditional instruments [1]. Concentric Tube Robots (CTRs) are representative continuum robots that exhibit shape change by the relative translation and rotation of precurved elastic tubes, telescopically inserted into each other. CTRs were originally envisioned as "single-arm" robots [2],[3] but are nowadays also considered as parts of "multi-arm" systems for surgical procedures (*e.g.*, in the prostate [4] or brain [5]).

Although mechanics-based models have been developed that can describe the shape of a single CTR of any number of tubes and different precurvatures [6, 2], limited work on multi-arm CTRs and their modelling has been performed. Contrary to prior work that considers the backbone that houses multiple robotic arms as stiff and "decoupled" from the motion of the flexible arms [7, 4], the proposed work accounts for the interactions between an arbitrary number of CTR arms and the flexible backbone. The theory is developed for a multi-arm continuum robot comprising a flexible CTR backbone that houses several CTR arms as end-effectors (see Fig. 1).

MATERIALS AND METHODS

The robot that motivates the modeling research is being designed for optic nerve glioma applications. It is envisioned that it will navigate peri-ocularly to reach the optic nerve. The backbone CTR is a 3 Degree-of-Freedom (DoF) variable stiffness section, comprising two precurved tubes. It is a "navigation section" providing global positioning for two flexible instruments and a camera. The arms act as "manipulation sections", carrying the end effectors for tissue manipulation and lesion treatment. Each robotic arm comprises two tubes, *i.e.* 4 DoFs. A filling material is placed inside the navigation section to retain the separation of the flexible manipulation sections within the robot's navigation backbone (see Fig. 1). The filling material is required to avoid contact between the CTR arms and ensure continuous contact between the manipulation arms and the navigation arm.

To develop the theoretical model for a multi-arm CTR as an eccentric arrangement of multiple CTRs, the Cosserat rod theory is employed with the assumptions of the classical elastic-rod theory of Kirchoff [6]. To get the shape of each tube, a set of differential equations, with kine-

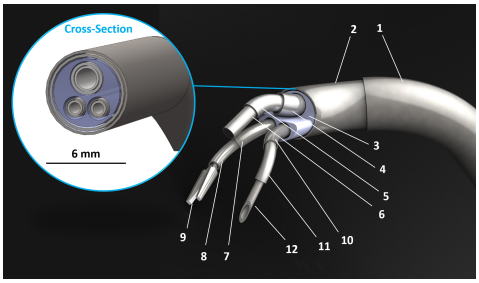

Fig. 1: Main components and architecture of the proposed microsurgical robot: (1) Main Body (MB) - Outer Tube (OT), (2) MB - Inner Tube (IT), (3) MB - Filling Material, (4) Camera Holder (CH) - OT, (5) CH - IT, (6) Camera head with integrated illumination, (7) Right Instrument (RI) - (OT), (8) RI - IT, (9) RI - end-effector, (10) Left Instrument (LI) - OT, (11) LI - IT, and (12) LI - end-effector.

matic variables the curvature of a referred tube and the torsion of each tube, are integrated simultaneously. The shape of each tube is determined by the position vector $\mathbf{r}_i^j = \mathbf{r}_i^j(s)$, where the coordinate $s \in [0, \ell]$ is the arc length, and ℓ is the tube's length and the rotation matrix of the frame moving along the tube's arc, $\mathbf{R}(s)$. Subscript i denotes the parameters and variables of the ith tube, while j denotes the section of the robot that the equation is referred to. For simplicity and without loss of generality, we present the model for the designed robot, *i.e.,* $i = \{1,2\}$ (two tubes per section, 1 denoting the inner tube, and 2 denoting the outer tube), and $j = \{1,2,3,4\}$ $(1-3$ for the manipulation sections and 4 for the navigation section). As the local curvature of a tube is obtained as $\mathbf{u}(s) = (\mathbf{R}^T(s)\mathbf{R}'(s))^\vee$, its shape can be computed by integrating $\mathbf{r}'(s) = \mathbf{R}(s)\mathbf{e_3}$ and $\mathbf{R}'(s) = \mathbf{R}(s)\hat{\mathbf{u}}$ where $\hat{\mathbf{u}}$ is a skew symmetric matrix. To preserve shape continuity, we "break" the robot into segments linking transitions points. Each transition point denotes the position where a tube goes from straight to curved or where a tube ends as is depicted in Fig. 2. The continuity of shape and internal moment must be enforced at each transition point. In our approach, we estimate the shape of each section in each

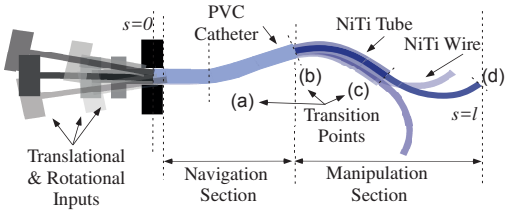

Fig. 2: Illustration of the concentric tube manipulation arms and the material filling the navigation section.

segment based on the deformed shape of a tube of reference. Without loss of generality, it is assumed that the navigation section 4 is the reference section for the segment that includes all tubes.

The twist of each tube is expressed with respect to the outer tube of the navigation section by introducing the angle $\theta_i^{(j)}(s)$ to parameterize tubes' twist. As a result every rotation can be expressed in relation to that tube taking also into account the eccentricity as

$$\begin{aligned} \mathbf{R}_{i=1,2}^{(j=1,2,3)} &= \mathbf{R}_{i=2}^{(j=4)} \mathbf{R}_{\phi}^{(j)} \mathbf{R}_{\theta_{i=1,2}}^{(j=1,2,3)} \\ \mathbf{R}_{i=1}^{(j=4)} &= \mathbf{R}_{i=2}^{(j=4)} \mathbf{R}_{\theta_{i=1}}^{(j=4)} \end{aligned} \tag{1}$$

where $\mathbf{R}_{\phi}^{(j)}$ is the rotation matrix that expresses the eccentricity of the outer tube of each manipulation arm with respect to the outer tube of the navigation section frame. By taking derivatives of the force and moment balances with respect to s and then by using a linear constitutive law we obtain derivatives of the kinematic variables:

$$\begin{aligned} \mathbf{u}_2^{\prime(4)}\Big|_{x,y} = -\mathbf{K}^{-1} \sum_{i=1}^{n} \mathbf{R}_{\kappa} \Big(\mathbf{K}_i^{(j)} \Big(\theta_i^{\prime(j)} \frac{\mathrm{d}\mathbf{R}_{\theta_i}^{T(j)}}{\mathrm{d}\theta_i^{(j)}} \mathbf{R}_{\phi}^{T(j)} \mathbf{u}_2^{(4)} - \mathbf{u}_i^{\prime *(j)} \Big) \\ + \hat{\mathbf{u}}_i^{(j)} \mathbf{K}_i^{(j)} \big(\mathbf{u}_i^{(j)} - \mathbf{u}_i^{*(j)} \big) \Big|_{x,y} \\ - \mathbf{K}^{-1} \Big(\mathbf{e}_3 \times \mathbf{R}_2{}^{T(j)} \int_s \mathbf{f}_s(\sigma) \mathrm{d}\sigma + \mathbf{R}_2{}^{T(j)} \mathbf{l} \Big) \Big|_{x,y}, \end{aligned} \tag{2}$$

where $\mathbf{K} = \sum_{i=1}^{n} \mathbf{K}_i^{(j)}$ and $\mathbf{R}_{\kappa}$ for the manipulation sections is $\mathbf{R}_{\kappa} = \mathbf{R}_{\phi}^{(j)} \mathbf{R}_{\theta_i}^{(j=1,2,3)}$ and for the navigation section is $\mathbf{R}_{\kappa} = \mathbf{R}_{\theta_i}^{(j=4)}$. As far as torsion is concerned, it can be derived from the third component of the equation that describes the curvature for a single tube, [6],

$$\begin{aligned} u_{i,z}^{\prime(j)} = u_i^{\prime *(j)} + \frac{E_i^{(j)} I_i^{(j)}}{G_i^{(j)} J_i^{(j)}} \big(u_{i,x}^{(j)} u_{i,y}^{\prime(j)} - u_{i,y}^{(j)} u_{i,x}^{\prime(j)} \big) + \\ \frac{G_i^{\prime(j)} I_i^{(j)}}{G_i^{(j)} J_i^{(j)}} \big(u_{i,z}^{\prime(j)} - u_{i,z}^{(j)} \big) - \frac{1}{G_i^{(j)} J_i^{(j)}} \mathbf{e}_3 \mathbf{R}_i^{T(j)} \mathbf{l}. \end{aligned} \tag{3}$$

All equations are integrated simultaneously together with the equations that describe the change of the transformation matrix along the length of the tube. Based on the expression of the curvature of each tube to the outer one, the rest curvatures can be obtained.

RESULTS

To evaluate the developed theory, the experimental setup shown in Fig. 3 was developed. The setup mimics the behavior of the proposed robot and has a single manipulation arm, placed eccentrically with respect to the navigation backbone longitudinal axis. The multi-lumen catheter is made of Polyvinyl Chloride (PVC) and emulates the flexible navigation section with its filing material. The manipulation arm is composed of a NiTi tube and a NiTi wire. To measure the shape of the tubes, two orthogonally arranged cameras observing the robot workspace from the top and the side were used. Moreover, since the actual values for the moduli of the tubes and the wire are uncertain (for the NiTi they are listed as 28-83 GPa and for the PVC, the Young's modulus varies from 2.3 to 4.8 GPa) , a calibration process was followed by solving an optimization problem for the parameter set $P = \{E_i^j I_i^j\}$ that identifies the moduli that minimise the error between the experiment and simulation. It was found for the NiTi tube and wire that $E \approx 20$ GPa while for the PVC is $E \approx 2$GPa.

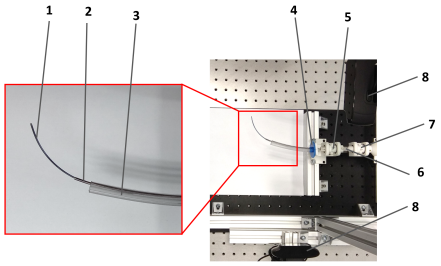

Fig. 3: Experimental setup: (1) Manipulation section - Instrument inner rod, (2) Manipulation section - Instrument outer tube, (3) Navigation section - PVC Multi-lumen catheter, (4) Catheter rotation control, (5), (6), (7) Rotation and translation control for the manipulation section, (8) Orthogonal cameras.

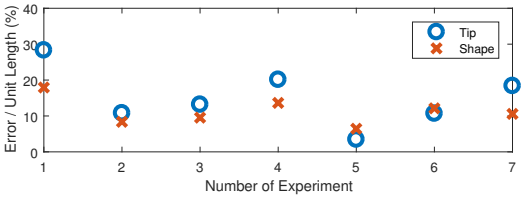

Fig. 4: Tip and shape error for 7 experimental trials.

In Fig. 4 the percentage of the error on the tip per unit length of the mechanism and the mean error in predicting the overall shape of the robot are shown. The average error per unit length on the whole shape is around 11%, which is reasonable for CTRs [6]. The sources of error in experimental data include the refraction caused by the PVC catheter, the camera calibration matrix, and triangulation of the selected points used to convert two 2D images into 3D shape of the robot.

REFERENCES

[1] J. Burgner-Kahrs *et al.* Continuum robots for medical applications: A survey, *IEEE Trans. Robot.*, 2015.

[2] P. E. Dupont *et al.* Design and control of concentric-tube robots, *IEEE Trans. Robot.*, 2010.

[3] A. Garriga-Cassanovas *et al.* Complete follow-the-leader kinematics using concentric tube robots, *Int. J. Robot. Res.* , 2018.

[4] R. J. Hendrick, *et al.* Hand-held transendoscopic robotic manipulators: A transurethral laser prostate surgery case study, *Int. J. Robot. Res.* , 2015.

[5] J. Burgner *et al.* A telerobotic system for transnasal surgery, *IEEE/ASME Trans. Mech.*, 2014.

[6] D. C. Rucker, *et al.* A Geometrically Exact Model for Externally Loaded Concentric-Tube Continuum Robots, *IEEE Trans. Robot.*, 2010.

[7] J. Ding, *et al.* Design and Coordination Kinematics of an Insertable Robotic Effectors Platform for Single-Port Access Surgery, *IEEE/ASME Trans. Mech.*, 2013.